Advances in Science and Technology Research Journal

Advances in Science and Technology Research Journal 2024, 18(4), 191–215
https://doi.org/10.12913/22998624/188819
ISSN 2299-8624, License CC-BY 4.0

Received: 2024.03.13
Accepted: 2024.05.17
Published: 2024.06.20

Mechanical Properties of Carbon Fiber Reinforced Materials for 3D Printing of Ankle Foot Orthoses

Justyna Rybarczyk[1*], Filip Górski[1], Wiesław Kuczko[1], Radowsław Wichniarek[1], Sabina Siwiec[2], Nikola Vitkovic[3], Răzvan Păcurar[4]

[1] Faculty of Mechanical Engineering, Poznan University of Technology, ul. Piotrowo 3, 60-965 Poznan, Poland
[2] Department of Computer Science and Statistics, Poznan University of Medical Sciences, ul. Fredry 10, Poznan, Poland
[3] Faculty of Mechanical Engineering, University of Niš, Univerzitetski trg 2, Niš 18000, Serbia
[4] Department of Manufacturing Engineering, Faculty of Industrial Engineering, Robotics and Production Management, Technical University of Cluj-Napoca, Blv. Muncii, No. 103-105, 400641 Cluj-Napoca, Romania
* Corresponding author's e-mail: justyna.rybarczyk@doctorate.put.poznan.pl

ABSTRACT

The article presents analysis of mechanical properties of specimens fabricated by fused deposition modelling (FDM). The four of considered materials are the well-known 3D printing filaments i.e., polylactide (PLA), Nylon 12 (PA12), acrylonitrile butadiene styrene (ABS), polyethylene terephthalate glycol (PET-G). The other four materials considered are carbon-fiber composites not described in the literature, i.e. polylactide with carbon fiber (PLA-CF), Nylon 12 with carbon fiber (PA12-CF), acrylonitrile butadiene styrene with carbon fiber (ABS-CF), polyethylene terephthalate glycol with carbon fiber (PETG-CF). The paper describes how the specimens were designed, printed, subjected to static tensile tests and static bending tests, and examined using microscopy. The obtained data uses to select the optimum material for the rapid manufacturing of lower limb orthoses. Carbon composites were found to have better mechanical properties of their base material, but the fabrication of composite samples is much more time consuming, for the reason that the manufacturing process is not stable.

Keywords: 3D printing, composites, ankle foot orthosis, additive manufacturing, carbon fiber, polymers.

INTRODUCTION

The rapid development of additive manufacturing, or additive molding (AM) technology, also known as 3D printing, makes it possible to shape parts with complex geometries and allows a significant reduction of the time required to produce a new product. The additive manufacturing process enables the creation of physical, three-dimensional (3D) shapes of almost any complexity stored in a CAD model [1, 2]. The wide spectrum of variations of additive manufacturing makes, it gives the possibility to produce parts from different types of materials. Compared to traditional technologies (casting, machining, plastic molding), AM has several significant limitations related to performance and quality, and most importantly, chemical and mechanical properties [2]. As per the ASTM F2792-12 standards [63], additive manufacturing (AM) is defined as the process of assembling materials to create objects from 3D model data, typically layer by layer, as opposed to subtractive manufacturing methodologies. Increasingly, the FDM additive manufacturing method is being used to manufacture medical devices. From a 3D-CAD data set, components and assemblies are fabricated from thermoplastic material in just a few work steps. Native software automatically slices the data, calculates support structures and creates tool paths. The parts are then built layer by layer using an additive process. The head extrudes molten thermoplastic

filament, to create each layer with a specific tool path. Through thermal fusion, the material fuses with the layer below it and solidifies. This creates a permanent bond between the two layers [3]. Composites of thermoplastic materials [4, 5] and FRP composite's [65] are increasingly being used in 3D-printing.

FDM technology in medicine

FDM printing has many advantages, the most important of which are: high strength of prints, a wide range of materials to work with, low cost of a single part, and the ability to print prototypes of mechanisms to test their functionality [18, 19]. Moreover, FDM technology can be used to create parts without geometric constraints, and there is no need for drilling or other machining operations [8, 64]. Finally, it is possible to eliminate or reduce residual stresses. Initially, the method was used to create low-cost prototypes and conceptual models. Today, it is being used to print high-quality functional prototypes and concept models. An important advantage is that models can be designed as cellular structures, such as honeycomb structures, which strengthen the part but reduce its weight. This is crucial when such fabricated manufacturing or assembly tools are operated by human workers [22]. Components made from these plastics can be as strong as their metal counterparts, but have less weight [23, 64]. By using special filaments, it is possible to **a**chieve comparable strength, impact strength and stiffness with less material density. Some 3D printing plastics have sufficient properties to produce parts that are traditionally made of metals. In addition to high strength, they are resistant to a variety of chemicals, including lubricants, and can be certified as non-flammable or bio-compatible. In the rapid manufacturing of custom polymer parts, there is no need to prepare an expensive mold, as is required for casting or injection molding [21].

Anatomical models are used in medical practice in many fields. Among the most important, it is worth mentioning preoperative and intraoperative support. In addition, models are an excellent tool for training in surgical procedures or learning about specific types of pathology at the level of patient and family education or for less experienced residents and medical students. Due to the relatively low cost of producing anatomical models, especially with FDM, the use of anatomical models at various stages of medical practice is possible and readily available. This is evidenced by the preoperative models presented:

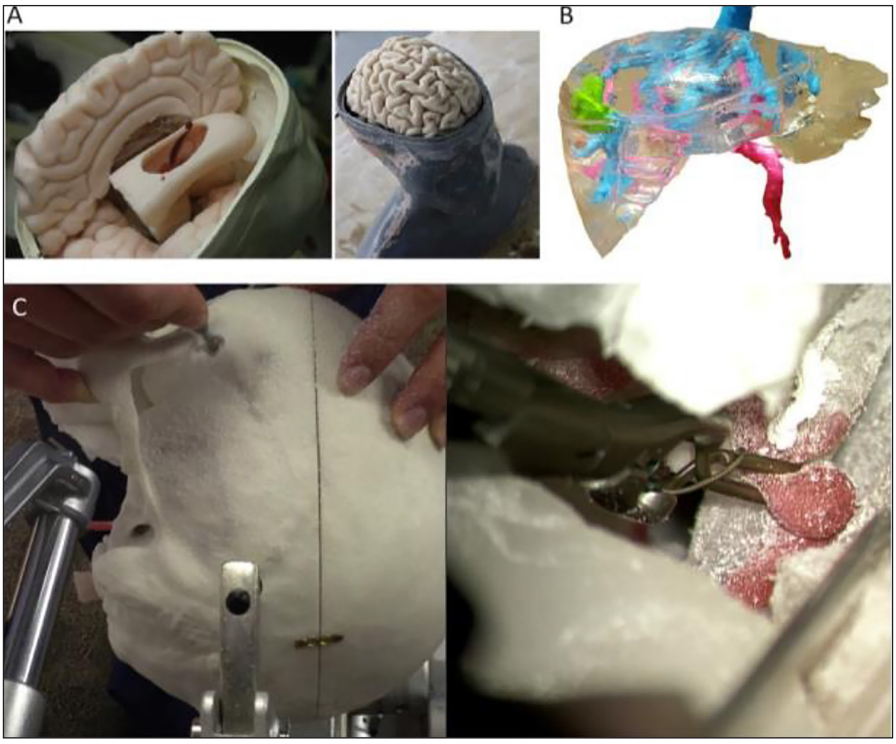

Figure 1. Example of the use of physical models in medicine: (a) endoscopic third ventriculostomy surgical simulator [6], (b) model for liver preoperative planning [7], (c) simulated surgery on the skull [8]

endoscopic third ventriculostomy surgical simulator [6] (Figure 1a), a model for perioperative planning of the liver [7] (Figure 1b), a model for simulating surgery on the skull (Figure 1c) [8], and a multi-material model of the kidney [9, 10].

Another example of the application of 3D Printing in orthopedics is wrist and upper limb prostheses (Figure 2), the process of which is fully automated using AutoMedPrint (automated 3D printing of medical products) and the price is several times lower than traditionally manufactured orthoses [13, 14]. There is already information in the literature about the possibility of obtaining a usable and inexpensive 3D-printed hand orthosis (shown in Figure 3) in less than one working day, from measurement to finished product, with minimal human operator involvement (e.g., using the AutoMedPrint system) and minimal competence required to carry out the entire process [13].

However, FDM can have some disadvantages. For example, the high anisotropy of 3D printed objects with respect to their internal structure [24, 25] makes it difficult to control their printing time or their mechanical properties and surface texture, such as roughness or waviness, depending on the technology used [26, 27, 28]. The mechanical properties of FDM-printed parts made of pure thermoplastic materials can be improved by using, for example, carbon-fiber or glass-fiber reinforcement [29, 30] and/or special additives whose role is to improve mechanical properties [31]. Carbon fiber reinforced composites have excellent mechanical properties, being stiffer and more resistant to impact and fatigue. Due to the low density of carbon fiber, all these properties can be achieved with low product weight. The use of carbon fiber or in selective laser sintering (SLS) contributes to the higher strength of the fabricated parts [32, 33].

Since the beginning of the 21st century, researchers have been searching for the relationship between various parameters of the FDM

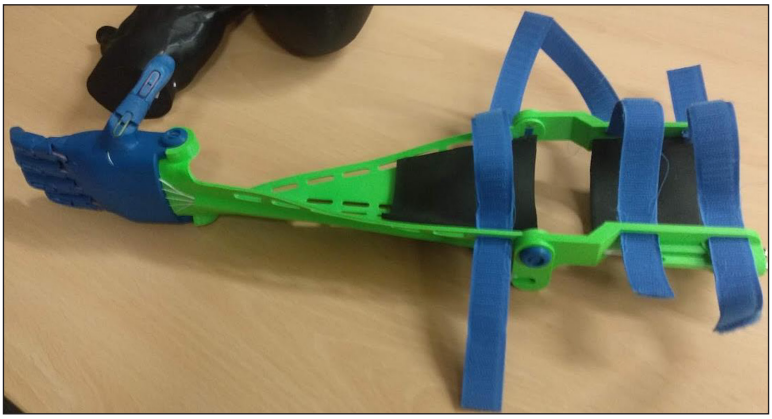

Figure 2. 3D printed complete mechanical prosthesis for patient [14]

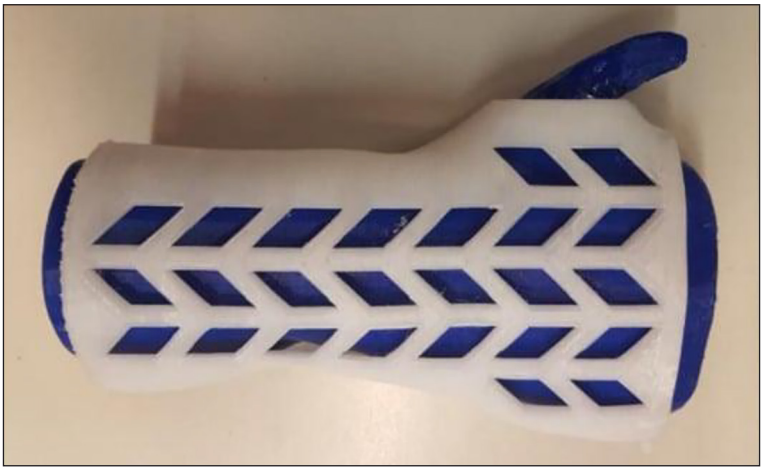

Figure 3. Orthosis on a two-material forearm phantom [13]

process and the strength of the resulting models. A number of research centers around the world are engaged in this kind of research. This group can include, among others, the work carried out by a group of scientists from Korea in cooperation with the University of Berkeley [36, 37]. These works show that there are problems with the one with FDM, so they focus primarily on the variation of parameters that determine the structure of the interior of the layers, i.e. how the layers are filled.

The main limitation of the plasticized plastic modeling technique is its low accuracy in the vertical direction, related to the relatively large layer thickness. This is related to the formation of the so-called stair-step effect, which occurs in all products manufactured with incremental techniques. This effect is related to the discrete division of the object into layers. In the FDM technique, it is particularly noticeable and, especially in the case of curvilinear outlines and free surfaces, affects the visual quality of manufactured products [38]. Another major limitation of FDM is the varying and not always favorable mechanical properties of products made with it. These properties should be assessed as good in comparison with other incremental manufacturing techniques, but it is worth noting that, for example, the tensile strength of products manufactured by the plastic incremental forming technique never reaches a level higher than 80% of the strength of the base material, and is usually much lower (2–3 times), and is also strongly dependent on the process parameters [38, 39, 40]. The orientation of manufacturing in FDM affects impact strength with pronounced anisotropy, and this is particularly noticeable with thicker layers. The effect of layer thickness on impact strength due to build orientation was different for flat and edge specimens. In the case of flat specimens, the impact load was parallel to the adjacent layers and it was the layers that withstood most of the applied load. Greater layer thickness promotes greater impact strength [41].

3D-printing of AFOs

FDM is being used in orthopedics as a replacement for traditional orthoses or prostheses. In 2021, the authors produced the first pair of lower extremity orthoses for a pediatric patient with spina bifida. Specialized orthoses used on a daily basis did not allow the patient to use them in bodies of water. Figure 4 shows their replacement, manufactured using the FDM method from thermoplastic material, allowing them to be used during swimming pool activities [12]. The FDM method has also been used to protrude a fully personalized ankle foot orthosis for the 11-year-old patient shown in Figure 5.

Ankle joint orthoses (AFOs) can be used in the treatment of many injuries, such as in children with cerebral palsy, as AFOs correct the ankle joint and neuromuscular buildup, in the case of a flat foot, in the case of an unstable ankle foot (e.g., after an ankle sprain) [42]. In order to obtain

Figure 4. AFO type orthoses used during pool activities

Figure 5. Personalized AFO orthosis

a personalized AFO, the following steps should be followed: measuring the ankle joint along with the patient's foot, making a positive plaster model using a casting technique based on the negative plaster impression, modifying the positive plaster model to fit the patient's anatomy, then making a vacuum deformation and fitting the orthosis. The process of the traditional approach is very labor-intensive, in addition to carrying many design limitations, as well as high costs and long waiting times [43, 44]. These downsides have led researchers to explore new techniques for manufacturing individualized AFO orthoses [45, 46]. Decades of development to replace conventional AM methodologies have resulted in a variety of manufacturing methods in which the component is fabricated layer by layer directly from a digital model. Layer by layer directly from the digital model [47, 48]. The use of the FDM method in the manufacture of orthopedic products, combined with 3D scanning technology, aims to eliminate the drawbacks of traditional manufacturing methods indicated earlier.

Different from the upper limb, the fabrication of ankle orthoses can be problematic. The orthoses have low strength and impact strength, the literature reports that the broken part of the orthosis shows that the direction of separation was not in the direction of 3D printing path deposition. This means that the printing pattern of each layer is also a key issue for the strength of the 3D printed object [47]. The age of the patient is also an important aspect, adults or older children should be designed with a heavier orthosis (Figure 6b) to prevent damage to the AFO, as in Figure 6a [13] FDM is therefore often abandoned in favor of more expensive and less accessible SLS or MJF techniques [50].

The potential use of polymer based composite materials could provide a solution to these strength problems, quite a few solutions can be found in lite-rature using composite filaments, which prove that the addition of carbon fibers

Figure 6. (a) An orthosis with a lighter design that broke during use, (b) an orthosis with a monolith construction

increases the stability and stiffness of the product [51]. Other possibilities include aramid fiber-reinforced [52], graphene-reinforced [53] and CFRTP [54] materials. Attention is also paid to the aspect of biocompatibility, as well as biodegradability, which have already been reported in the literature [16, 55]. There are already successful applications of biodegradable composites in orthopedics [16, 56], as well as polymer-based carbon fiber composites [5].

The following article is the first stage of research aimed at determining experimentally the geometric and technological parameters that enable the requirements for the mechanical, functional and therapeutic properties of AFO orthoses, manufactured incrementally on the basis of an automatically generated design, while meeting the condition of low price and rapid delivery of the product to the patient.

MATERIALS AND METHODS

Research concept and plan

The overall goal of the ongoing research is to determine by experimental method whether the strength properties of the carbon fiber composites are good enough to use them to manufacture functional AFO orthoses. The research is part of the project "Automation of design and rapid manufacturing of individualized orthotic and prosthetic products based on data from anthropometric measurements" and "Determination of technological parameters and properties of selected incrementally manufactured orthopedic products". The orthosis were designed and manufactured in 3D using the AutoMedPrint system. The main stages of using the system are: 3D scanning of patient limb, automated data processing, automated CAD design of a selected product (based on 3D scanning data), semi-automated preparation of 3D printing process and its realization, and fitting with the patient. The principle of operation of the AutoMedPrint system is shown in Figure 7 [12, 43].

The main aim of the research is to improve the production process of customized ankle foot orthoses in the AutoMedPrint system by enabling new material choices and assuring that the produced orthoses will meet all the evaluation criteria stated in the available standards [ISO 13485:2016]. Basing on the available literature, it was proposed to utilize composite materials as basic materials for building the orthosis shell - potentially overcoming the strength barriers observable while using standard thermoplastic polymers. As such, a series of experiments were proposed in order to verify if the carbon-fiber filled thermoplastic materials will prove to be more durable, while maintaining the acceptable accuracy, as well as low manufacturing cost and short time of manufacturing using the widely available FDM technology.

The tests were carried out on four pairs of typical FDM materials (ABS, PETG, PA12, PLA) and their composites with the addition of CF (ABS + CF, PETG + CF, PA12 + CF, PLA + CF). The printed specimens were subjected to non-destructive testing - roughness testing and microscopic structure testing, as well as destructive

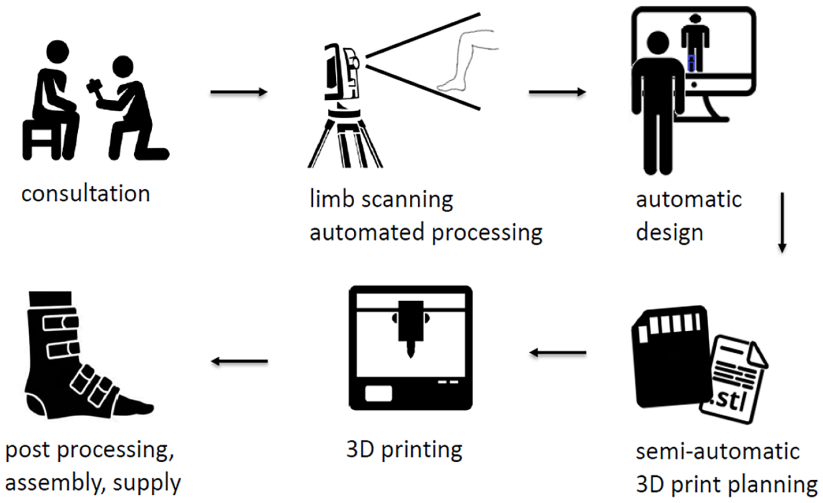

Figure 7. The principle of operation of the AutoMedPrint system

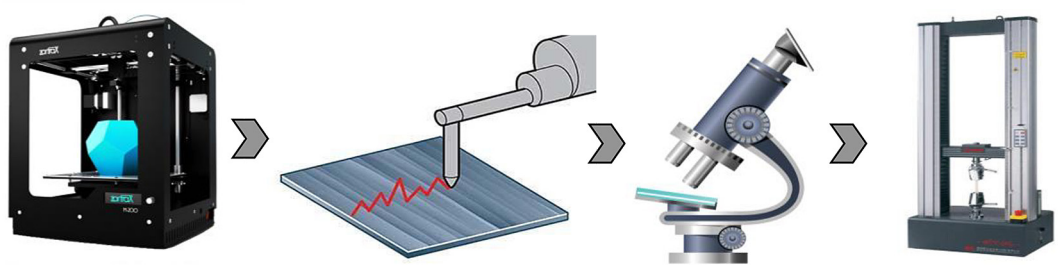

Figure 8. Testing process: (a) 3D printing, (b) roughness testing, (c) microscopic imaging, (d) static strength testing

testing – static tensile testing. The testing process is shown in Figure 8.

Characteristics of used materials

In the realized study, four types of the most commonly used materials and their composites for 3D printing: PLA, PET-G, ABS, and PA12 were tested. Only commercially available materials were considered, with wide availability and potentially low or medium price (to maintain the low-cost production aspect of the AutoMedPrint system, in accordance with research goals and concepts). The first material used in the study was PLA and its composite PLA with carbon fiber. Polylactide (PLA) is the most extensively researched and utilized biodegradable and renewable aliphatic polyester [57], widely popular in the FDM technology, due to its low thermal shrinkage, allowing to realize stable layer deposition process on most machines available on the market, including the cheapest ones.

Moreover, PLA has many advantages, which include:

- environmental friendliness – in addition to being derived from renewable raw materials (e.g. corn, wheat), PLA is biodegradable, recyclable, compostable [57];
- biocompatibility – the most attractive aspect of PLA, especially for biomedical applications. A biocompatible material should not cause toxic or carcinogenic effects in local tissues. In addition, degradation products should not interfere with tissue healing [57].

PLA (Spectrum premium filaments, Spectrum Group, Sosnowiec, Poland) and PLA-CF (F3D filament, FINNOTECH, Katowice, Poland) filaments were used in the study. According to the manufacturer, the PLA-CF filament contained 15% carbon fibers.

ABS (acrylonitrile butadiene styrene) is a common thermoplastic that is amorphous in nature and has high impact resistance, heat resistance and toughness, low thermal conductivity. The high moulding behavior of ABS makes it one of the best thermoplastic for possible preparations of nano-porous material in energy conversion and storage units [58]. It is also a very popular material in FDM technology, although it requires machines with closed chamber and heated building table, to prevent disjoining of partially completed prints from the table as a result of thermal shrinkage. ABS (Spectrum premium filaments, Spectrum Group, Sosnowiec, Poland) and ABS-CF (KIMYA (HQ), Nantes, France) filaments were used in the study. According to the manufacturer, the ABS-CF filament contained 10% carbon fibers.

PA 12 (Polyamide 12) is one of the most resourceful materials in professional 3D printing. For its mechanical parameters, flexibility, and heat resistance, it is a great option for functional prototypes. Nylon 12 is chemical resistant and not sensitive to stress cracking [59]. In the FDM technology, PA12 is considered moderately difficult in processing, requiring closed chamber machines, with usually higher extrusion temperatures than ABS and PLA, as well as properly prepared table surface due to low adhesion and increased risk of disjoining during layer deposition process. PA12 (Fiberlab S.A., Brzezie, Poland) and PA12-CF (Fiberlab S.A., Brzezie, Poland) filaments were used in the study. According to the manufacturer, the PA12-CF filament contained 15% carbon fibers.

PET-G (Polyethylene Terephthalate Glycol) is another very popular material used in 3D printing processes. It has good elasticity and impact strength, compared with PLA and ABS. It is also easy in processing using the FDM technology, allowing to obtain a glossy surface of produced parts. It can be printed on most available machines, including low-cost ones.

PETG (ROSA 3D Filaments, Hipolitów, Poland) and PETG-CF (KIMYA (HQ), Nantes, France) filaments were used in the study. According to the manufacturer, the PETG-CF filament contained 10% carbon fibers. The basic properties of the selected materials are presented in Table 1. They have been taken from the characteristics supplied by their manufacturers.

Manufacturing of the ASTM standard sample

The manufacturing was realized using the 3D printer Zortrax M200 Plus (Zortrax, Olsztyn, Poland). The specification of the used 3D printer is presented in Table 2. The 3D-printed specimens (Fig. 9) of the selected materials were compatible with the ISO standard for testing the strength of polymer materials [ISO 527-1]. For static tensile testing, they were used the dogbone-shaped samples (Fig. 9a), while for the bending test, they were the rectangular beam samples (Fig. 9b). The samples were printed in the two series of 5 samples each. Figure 10 shows one of the series of printing of the ABS samples. Table 3 contains standard manufacturing parameters for all materials for the tensile test samples and bending test samples. Tables 4 and 5 show the manufacturing parameters for different materials for tensile test samples and bending test samples. The parameters' values were selected according to the recommendations of material and machine producers, as

Table 1. Characteristics of manufacturing data sheets of used materials

No.	Name	Properties
1	PLA	Density: 1.22 g/cm^3 Extrusion temperature: 185–230 °C Build platform temperature: 0–45 °C
2	PLA-CF	Density: 1.30 g/cm^3 Extrusion temperature: 255–270 °C Build platform temperature: 50–70 °C
3	ABS	Density: 1.05 g/cm^3 Extrusion temperature: 230–255 °C Build platform temperature: 100 °C
4	ABS-CF	Density: 1.045 g/cm^3 Extrusion temperature: 250–270 °C Build platform temperature: 90–110 °C
5	PA12	Density: 1.01 g/cm^3 Extrusion temperature: 255–270 °C Build platform temperature: 100 °C
6	PA12-CF	Density: 1.07 g/cm^3 Extrusion temperature: 265–270 °C Build platform temperature: 90–110 °C
7	PETG	Density: 1.29 g/cm^3 Extrusion temperature: 220–260 °C Build platform temperature: 60–80 °C
8	PETG-CF	Density: 1.28 g/cm^3 Extrusion temperature: 220–260 °C Build platform temperature: 60–100 °C

Table 2. Specification of Zortrax M200 Plus

Data sheet	
Technology	LDP/FFF
Working area	200×200×180 mm
Supported materials	M Series dedicated materials (recommended) + new Z-SEMIFLEX
Nozzle size	0.4 mm
Filament diameter	1.75 mm
Extruder	Single
Storage temperature	0–35 °C
Printer size (excluding spool holder)	350×360×505 mm
Cooling system	Double fan and extruder cooling

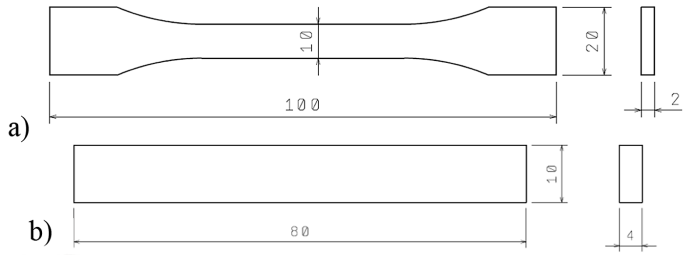

Figure 9. Dimensions of specimens for experimental strength tests: a) tensile test, b) bending test

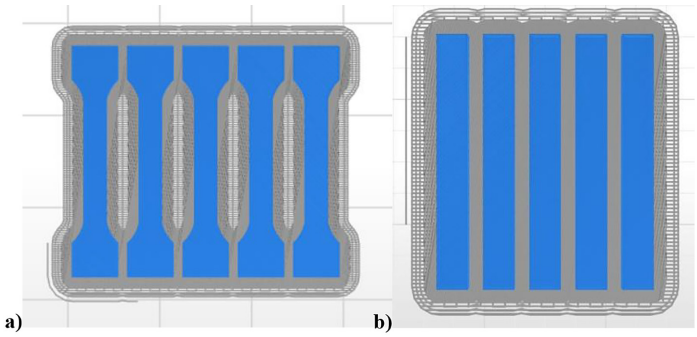

Figure 10. Samples from the Z-SUITE (ver. 2.26.0.0)) program: (a) tensile test, (b) bending test

Table 3. Standard manufacturing parameters for all materials and both sample types

Parameter	Value
Nozzle diameter [mm]	0.4
Layer [mm]	0.19
Fan speed	Auto
Contour-infill gap	0.4
Contour-top gap	0.25
Surface layers top	7
Surface layer bottom	4
Max. wall thickness [mm]	3.13

well as the experience of the team of authors, to ensure stable processes. Tables 6 and 7 present the estimated times and material consumption of the manufacturing of the tensile and bending test specimens calculated using the Z-SUITE program version 2.26.0.0.

Non-destructive testing methodology

Initially after manufacturing the samples, their quality was visually assessed to check if the shape was properly recreated and if there

Table 4. Manufacturing parameters for different materials – tensile test samples

Specification	ABS / ABS + CF	PETG / PETG + CF	PLA / PLA + CF	PA12 / PA12 + CF
First layer gap [mm]	0.32	0.47	0.49	0.45
Raft layers	8	4	5	4
Platform - raft gap [mm]	0.32	0.25	0.32	0.3
Support density [mm]	3.50	3.00	3.00	3.00

Table 5. Manufacturing parameters for different materials – bending test samples

Specification	ABS / ABS + CF	PETG / PETG + CF	PLA / PLA + CF	PA12 / PA12 + CF
First layer gap [mm]	0.32	0.43	0.49	0.43
Raft layers	8	7	5	5
Platform - raft gap [mm]	0.42	0.25	0.32	0.3
Support density [mm]	3.50	3.00	3.00	3.00

Table 6. Estimated times and consumption of material in the tensile test

Specification	ABS / ABS + CF	PETG / PETG + CF	PLA / PLA + CF	PA12 / PA12 + CF
Time	2 h 17 min	1 h 50 min	1 h 56 min	2 h
Material usage	10.8 m (26 g)	8.53 m (26 g)	9.33 m (27 g)	8.13 m (16)

Table 7. Estimated times and consumption of material in the bending test

Specification	ABS / ABS + CF	PETG / PETG + CF	PLA / PLA + CF	PA12 / PA12 + CF
Time	2 h 15 min	2 h 56 min	2 h 50 min	2 h 14 min
Material usage	8.47 m (20 g)	10.01 m (28 g)	10.66 m (30 g)	8.45 m (16 g)

are no major structural errors (resulting, e.g., from machine errors) which would heavily influence the further testing procedures. If such defects were identified, they were written down and a decision was made if such a specimen should be rejected and printed again or kept for further experiments. The digital microscope ISM-PM200SA (Insize Co., Ltd., Suzhou New Distric, China) was used to inspect the surface of the dogbone-shaped specimens to detect any surface defects or cracks that may affect the destructive test results. The digital microscope can provide high-resolution images of the specimen surface, allowing for the identification of even the smallest defects. After the digital microscope examination, the tensile test was performed on the specimens. Once the tensile test was complete, the specimens were again subjected to microscope testing, to visualize the fracture area and compare it for different materials. Figure 11 presents the course of the test. The second non-destructive test performed on the specimens was the roughness test. The roughness was tested by use of a certified roughness tester. All the specimens were measured with the PowerSurf ART-300 Surface Roughness Tester (PowerTech s.c., Grojec, Poland). The device is compatible with appropriate EN ISO 4287 and EN ISO 4288 standards. The fracture surface was measured, which can provide valuable information about the material's fracture behavior. The roughness test was performed on both the tensile and bending samples, only after the destructive testing. The measurements were made along a constant distance of 2.5 mm, with a velocity of 1 mm/s, in locations presented in Figure 12a and 12b. Three repetitions were performed for each sample. Figure 12c presents the course of the test.

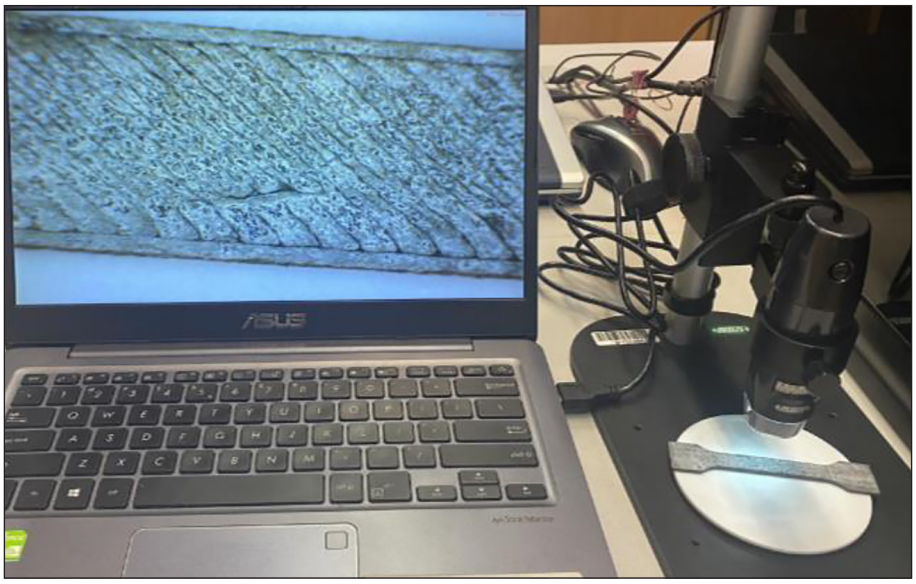

Figure 11. Procedure for testing the tensile test sample using the microscope

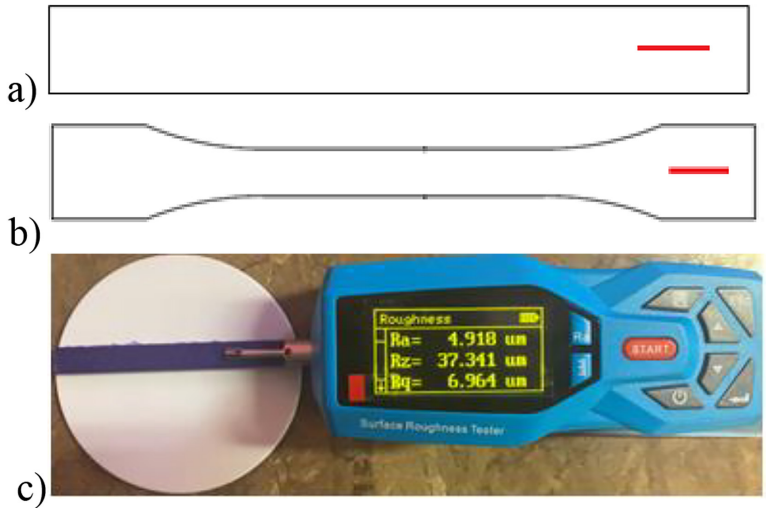

Figure 12. Places where the roughness measurement was carried out, sample type: a) bending, b) tensile; c) roughness testing on the bending test specimen

Figure 13. Test setup – tensile test

Methodology of destructive testing

Strength measurement was realized using a Universal Testing Machine (SUNPOC, Guiyang, China) at room temperature and a crosshead speed of 20 mm/min. To ensure accuracy and reproducibility, ten samples of each type were tested. A picture illustrating the test setup is shown in Figure 13. After the samples were prepared, they were attached to the grips of the universal testing machine. The grips were adjusted and tightened to ensure a stable and secure grip on the specimen. The support spacing was set at l = 64 mm.

Next, a tensile test was carried out on the specimens. During the tensile test, the specimen was subjected to an increasing tensile load until it was broken. A universal testing machine measured the load applied to the specimen and, using the introduced specimen dimensions, stress and strain values were calculated automatically.

The bending test was performed by placing the specimen on the support of the universal testing machine and applying the load at the center

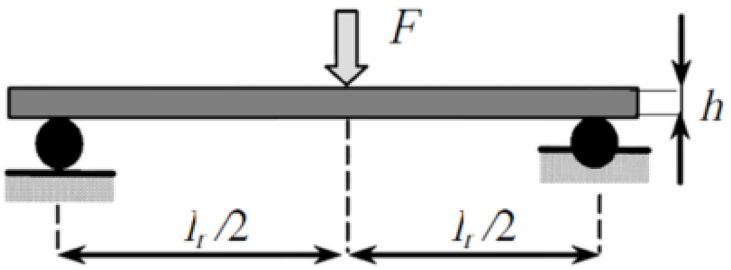

Figure 14. Test setup – three point flexure strength, h = 10; l = 64

of the specimen (Fig. 14), with the feed rate assumed 1 mm/min. The test was finished in one of two cases: when the sample fractured or when 10 mm of deflection was reached. In the bending test, the load applied to the specimen and the resulting displacement was measured, which was used to calculate the stress and strain values in bending.

RESULTS

Manufacturing results

The manufacturing of specimen was realized according to the assumed plan. All the specimens were acquired, although not without certain problems with process stability. The manufacturing errors that occurred were divided into two categories:

1. Major errors – they caused the specimens to be unusable in further tests, e.g. major shape errors, layer disjoint etc.
2. Minor errors – visible with the naked eye and possibly could have influenced the results of testing, but the main shape and function of the manufactured specimens was sustained. The minor errors are illustrated in the further part of the text with microscopic images, for clarity.

Regarding the specific material pairs (thermoplasts and their CF-filled counterparts), certain observations were made, described below. In the case of ABS material – the ABS-CF was the least stable and most problematic of all the materials considered in this study. 7 processes were required to obtain the complete set of samples for the tensile tests (2 batches per 5 specimen), which is a very low success ratio of ~30%. In the case of bending tests, it was a bit better, but the process was still not perfectly stable and the nozzle of the machine was regularly clogging. Here, adding CF had the biggest impact on process stability, as pure ABS was manufactured without any problems. However, pure ABS material samples had the most minor errors of all the materials. Examples of major errors while printing ABS-CF samples are shown in Fig. 15a, while minor errors of pure ABS are shown in Fig. 15b. In the case of PLA material – the pure PLA was very stable and the manufacturing was 100% successful (all the batches produced

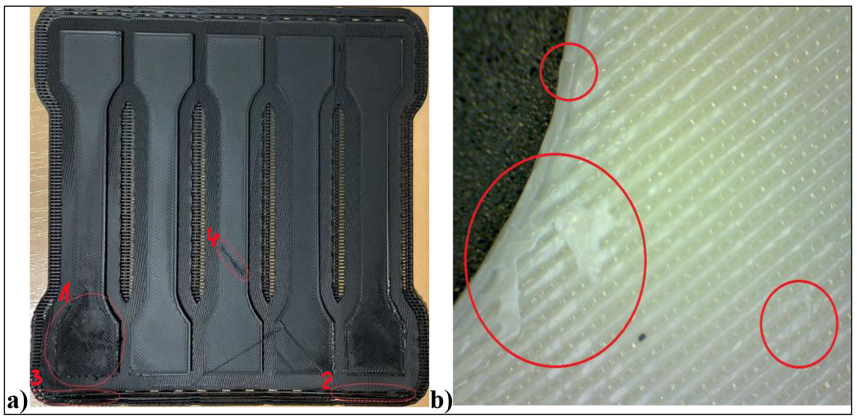

Figure 15. (a) Major errors of printing ABS-CF samples: (1) rolled up corner, (2) and (3) detachment of raft from the table, (4) underextrusion caused by clogging, (b) minor errors of printed ABS samples

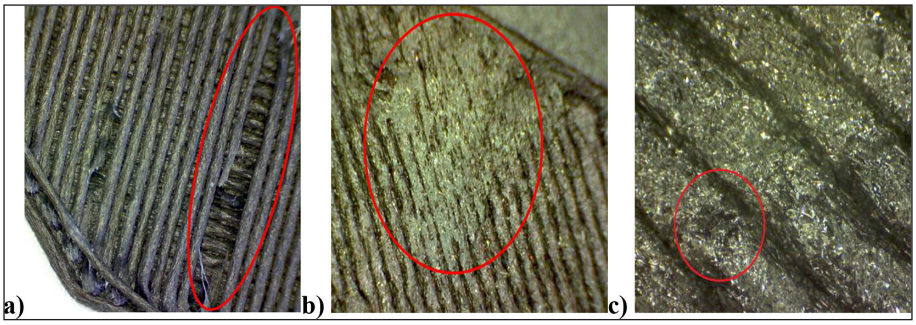

Figure 16. (a) Minor error of printed PLA-CF samples – lack of material thread, (b) minor error of printed PA12-CF samples, (c) minor errors of printing PETG-CF samples

at first attempt). Slight problems occurred with the PLA-CF material – 2 attempts at tensile test specimens manufacturing were unsuccessful (samples disjoined from the table mid-print, despite proper preparation of table surface and using recommended parameters), which gives a success ratio of 50% for this material. Similarly as in the ABS-CF, the nozzle was clogging regularly. Examples of minor errors in manufactured samples are presented in Figure 16a.

When manufacturing PA12 material no stability problems occurred, the printouts were not disjoining from the machine working table, no major errors were recorded (100% success ratio for both types of samples produced). However, nozzle clogging was also observed for the CF-filled material. Examples of minor errors in manufactured samples are presented in Fig. 16b. In the case of PET-G material – similarly as in the case of PA12, the processes both for pure and CF-filled material were generally stable, without major errors occurring. Examples of minor errors are shown in Fig. 16c. Tables 8 and 9 present estimated times and material consumption for two types of produced samples. It can be observed that the printing PETG and PETG-CF samples for tensile and bending tests took the longest time and the most amount of material was used in their manufacture. Time of printing tensile samples of ABS and ABS-CF was the shortest of all of used materials and composites, but PA12 and PA12-CF were used the least amount of material in their manufacture.

Time of bending samples of PA12 and PA12-CF was the shortest of all of used materials and composites, and the least amount of material was used in their manufacture. The bending samples of PA12 and PA12-CF were used the most amount of material in their manufacture. The actual times were exactly the same as predicted. The times were well estimated by the Z-SUITE program. This allowed a very good estimate of the real time necessary to produce all the samples. Post-processing for carbon fiber materials turned out to be much easier and therefore faster. Isolation of the raft from the specimens is done in one stroke and no more processing is required, because the specimens are already ready for testing, in contrast to samples from base materials, at which the raft breaks and has to be levered several times.

As a summary, it can be stated that the process of manufacturing samples from all composite materials, except ABS-CF is stable and there is no problem with printing the set product. Sample fabrication time oscillates around 2 hours for all materials except PETG-CF, for which this time is almost an hour longer. A significant difficulty in manufacturing carbon fiber composites is nozzle clogging and much faster (nearly 2.5 times) nozzle wear.

Destructive testing results

The results of tensile tests are presented in Tables 10 and 11. The tables contain both raw

Table 8. Estimated times and consumption of material in the tensile test

Specification	ABS / ABS + CF	PETG / PETG + CF	PLA / PLA + CF	PA12 / PA12 + CF
Time	1 h 50 min	1 h 53 min	1 h 56 min	2 h
Material usage	23.08 g / 23.53 g	29.22 g / 28.81 g	24.25 g / 25.24 g	18.14 g / 19.11 g

Table 9. Estimated times and consumption of material in the bending test

Specification	ABS / ABS + CF	PETG / PETG + CF	PLA / PLA + CF	PA12 / PA12 + CF
Time	2 h 15 min	2 h 56 min	2 h 50 min	2 h 14 min
Material usage	20.22 g / 20.84 g	30.34 g / 30.10 g	31.27 g / 31.55 g	18.32 g / 19.27 g

Table 10. Strength testing results – tensile test, pure polymer filaments

Material	F_{max} [N]	dL_{Fmax} [mm]	σ_{max} [MPa]	ε_{max} [%]
ABS	570.9	3.28	27.87	5.47
PLA	780.8	3	39.13	5.17
PA12	497.5	15.7	25.27	24.86
PETG	660.4	4.1	32.8	6.13

Table 11. Strength testing results – tensile test, polymer filaments with carbon fiber

Material	F_{max} [N]	dL_{Fmax} [mm]	σ_{max} [MPa]	ε_{max} [%]
ABS-CF	611	3.37	31.43	5.62
PLA-CF	511.5	5.42	23.51	9.03
PA12-CF	735.6	5.04	35.81	10.12
PETG-CF	906.1	3.45	45.61	5.18

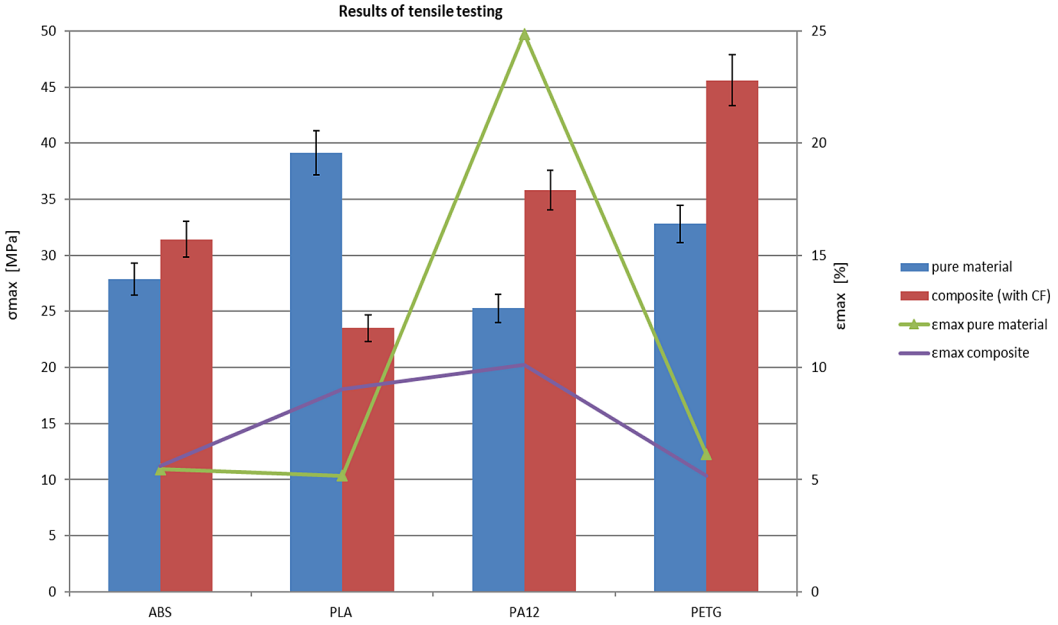

Figure 17. Results of tensile testing

data from testing machine sensors (forces and deflections), as well as calculated stress and strain values. Figure 17 presents juxtaposition of results contained in Tables 10 and 11. Figures 18a and 18b present example diagrams for pair of PETG and PETG-CF materials. Analyzing these results, the following observations can be made:

1. In the case of almost all tested materials, adding carbon fiber increased the tensile strength (maximum recorded stress). An adverse effect was obtained in the case of PLA material – here the tensile strength was lower – so composite material is actually worse in terms of recorded strength.
2. Considering the elongation, it almost did not change for the ABS material and slight change was observed for the PETG material (comparing pure and composite filaments). This is also reflected in the change of tensile strength values for these two pairs of materials. However, for PLA material, observable increase was registered when testing samples of composite, CF-filled filament – inversely to the change in tensile strength (so, for PLA, strength of CF-filled material is lower, but elongation is higher than in the case of pure polymer). The highest difference here is observed for PA12 – the elongation is much lower for composite material than for the pure material. Judging from both the diagrams (Fig. 17) and calculated values, it can be observed that pure PA12 is both more elastic and plastic than the same material filled with carbon fiber.
3. In the group of pure polymers, PLA samples had the highest tensile strength (with PETG ranked second). In the CF-filled materials, PETG has the highest tensile strength (with PA12 ranked second), while PLA is the last. Considering the relative increase in strength, PA12 and PETG benefitted the most from adding carbon fiber – their relative strength increase was approx. 40%. In the case of ABS, this increase is also observable (13%), but not as significant.

In Figures 19a, b and 20a, b, broken samples of PETG-CF, ABS-CF, ABS and PLA are presented. Analyzing the fractured samples, a general observation can be made, that all the samples, except

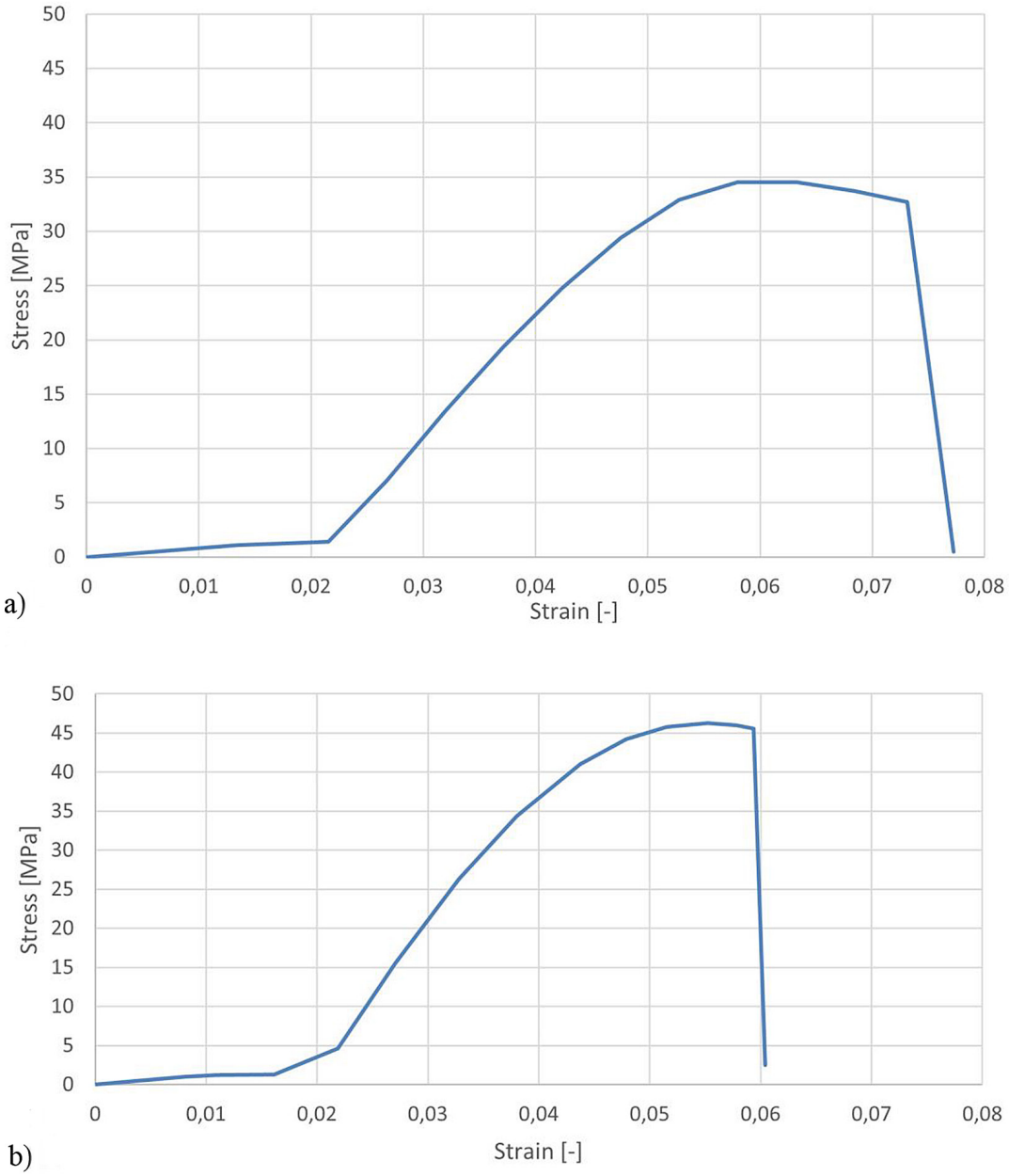

Figure 18. (a) Stress-strain diagram of PETG, (b) stress-strain diagram of PETG-CF

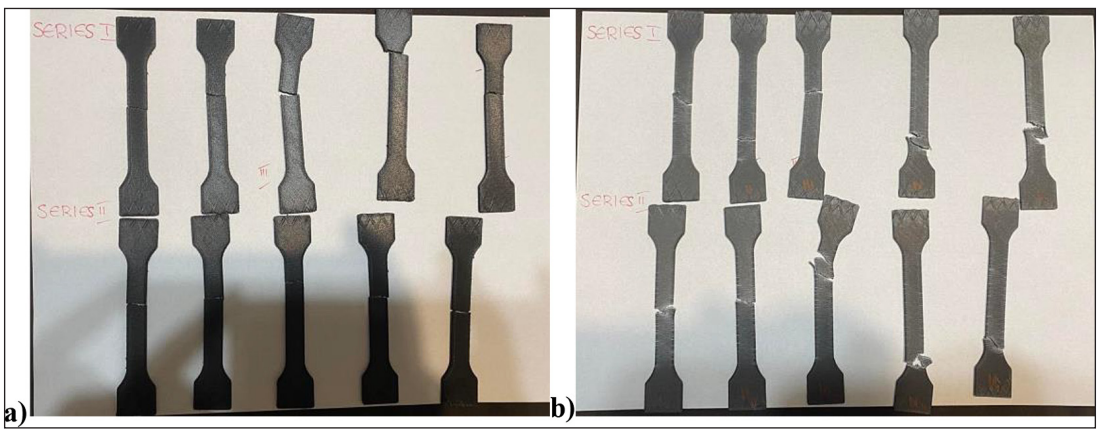

Figure 19. (a) Broken samples of PETG-CF, (b) broken samples of ABS-CF

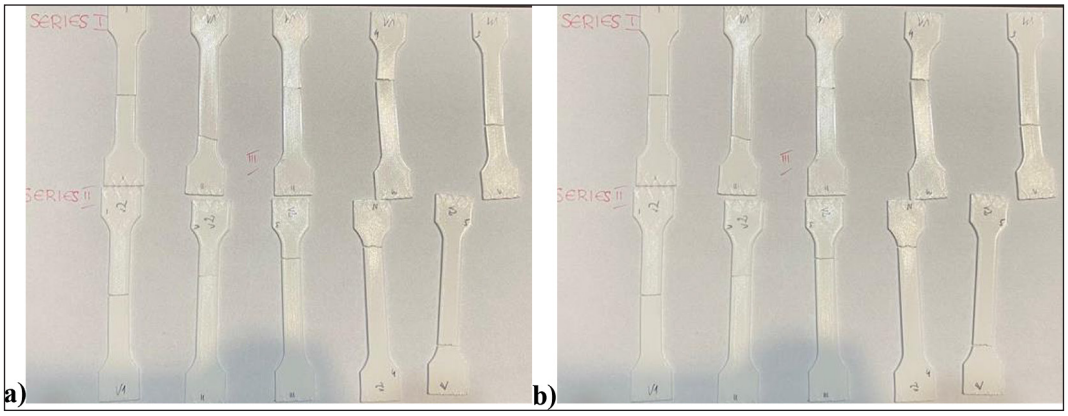

Figure 20. (a) Broken samples of PLA, (b) broken samples of ABS

ABS-CF, failed by layer disjoint (so-called "brittle fracture", characteristic for FDM printed parts), with no or little observable material deformation – the fracture surfaces are small and even at the macroscopic visual observation. For the ABS-CF, behavior was different, as presented in Fig. 19b – clear deformation of material threads is visible (with accompanying change of color). For all the other materials, no deformation is visible. The results of bending tests are presented in Tables 12 and 13. The tables contain both raw data from testing machine sensors (forces and deflections), as well as calculated stress and strain values. Figures 21a and b present example diagrams for pair of PA12 and PA12-CF. Analyzing these results, the following observations can be made:

- for two materials, adding carbon fiber actually reduced registered bending strength (measured as maximal stress during bending). For ABS, the reduction was very slight, but for PLA it was significant – approx. 50% of strength reduction. For the other two materials, notable increase in bending strength was observed;
- taking into account the deformation, in all four material pairs, CF-filled materials deformed slightly less than the pure polymers. The difference is visible mostly for PETG and PLA materials, with a very slight decrease for ABS and PA12. It means that the CF-filled materials are more rigid and less prone to bending, which is also visible when comparing loading diagrams from the machine (Fig. 21);
- as with the tensile test, for pure (non-composite) material group, PLA was the strongest one, with PA12 having the lowest maximum force and stress registered in the test. Considering the composite material group, the ranking is again different – PETG is apparently the strongest, with ABS the weakest, comparably with PLA. The two materials that benefit most from adding carbon fiber, in terms of raw strength (in both tests) are therefore PA12 and PETG.

Table 12. Strength testing results – bending test, pure polymer filaments

Material	F_{max} [N]	dL_{Fmax} [mm]	σ_{max} [MPa]	ε_{max} [%]
ABS	68.02	9.50	39.25	5.36
PLA	121.8	6	74.27	3.98
PA12	49.32	9.85	27.7	5.99
PETG	76.68	9.79	45.02	5.51

Table 13. Strength testing results – bending test, polymer filaments with carbon fiber

Material	F_{max} [N]	dL_{Fmax} [mm]	σ_{max} [MPa]	ε_{max} [%]
ABS-CF	66.78	9.57	37.34	5.22
PLA-CF	73	5.21	39.21	3.29
PA12-CF	78.64	9.91	48.77	5.7
PETG-CF	102.3	7.57	59.79	4.53

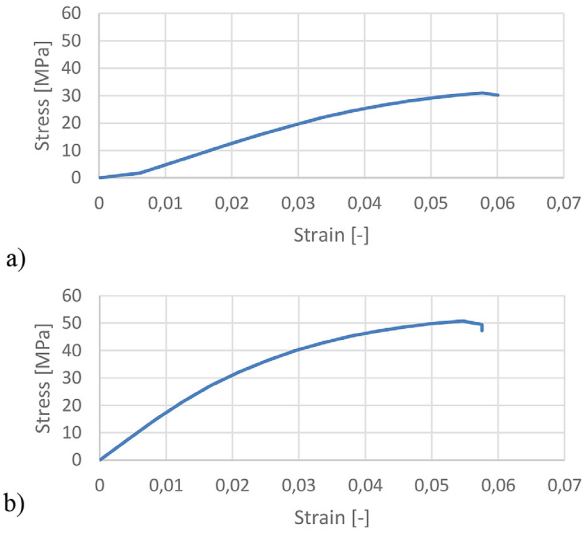

Figure 21. (a) Stress-strain diagram of PA12, (b) stress-strain of PA12-CF

Examples of samples after the test are presented in Figure 23. Due to a different nature of the test, no sample in bending test was damaged or failed, just heavily deformed, as in the case of PETG specimen visible in Fig. 23a. In the case of that particular specimen it can also be observed, that its deformation is asymmetric, despite load being put exactly in the middle of the sample. This could be caused by initial stress and microdamage caused during removal of the sample from the machine and support structure (raft) removal. In the case of other materials, the asymmetric deformation is also visible in some specimens, but not as clearly as in this example. Other causes of asymmetric deformation may include non-uniform distribution of carbon fibers in the material (when considering the CF-filled materials).

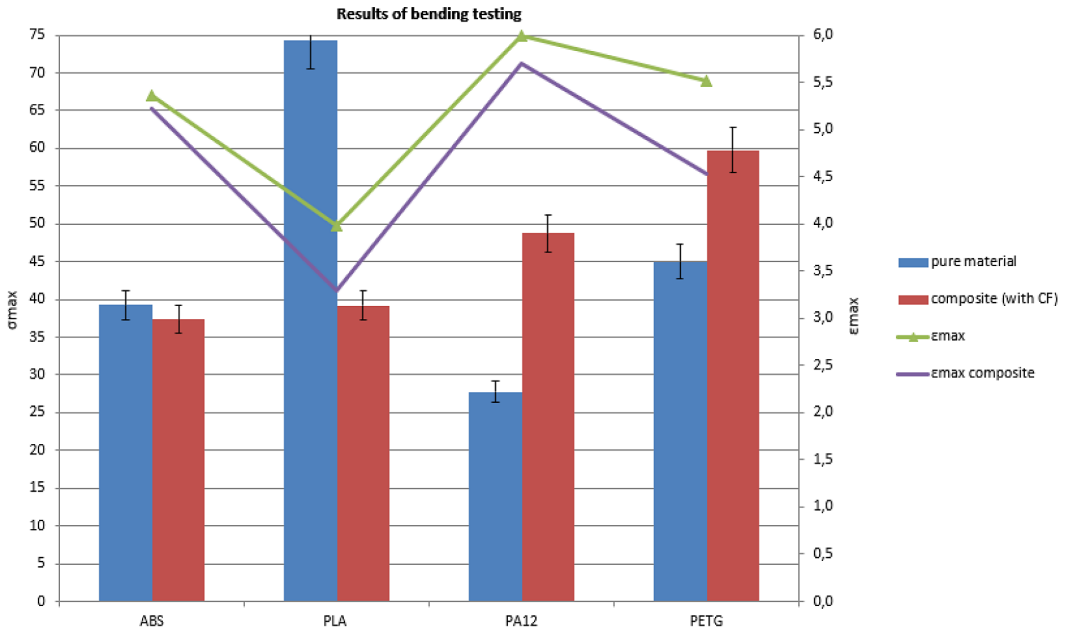

Figure 22. Results of bending testing

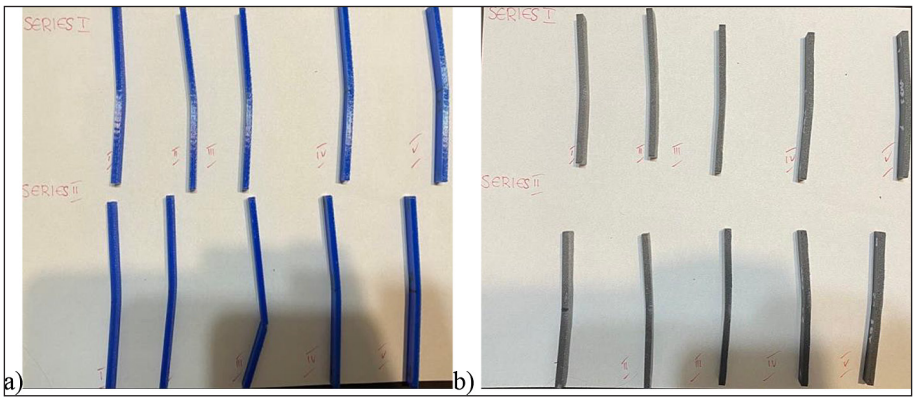

Figure 23. Examples of samples after the test: (a) PETG, (b) ABS-CF

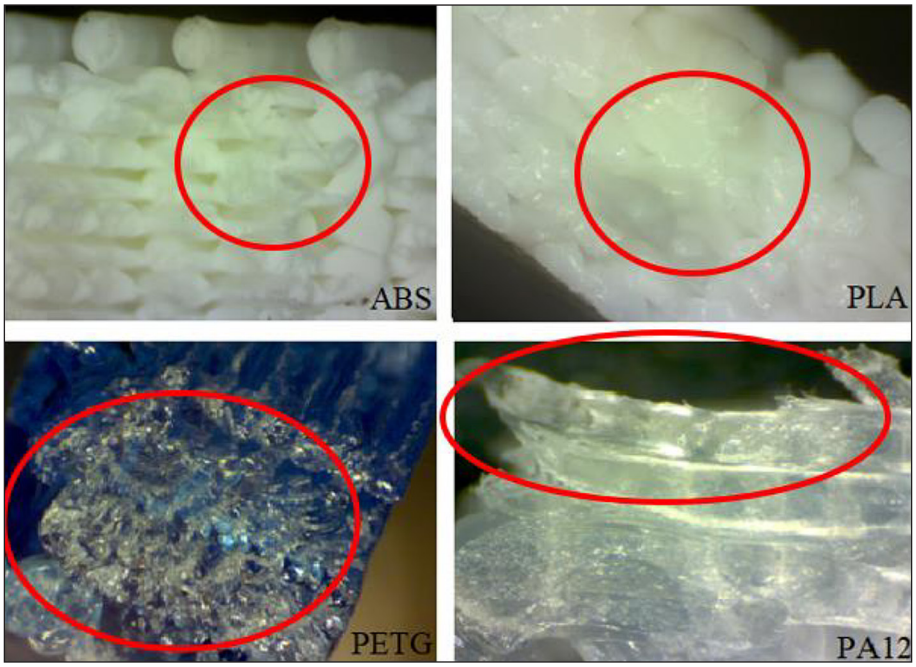

Figure 24. Microscopic imaging of pure polymer samples (after tensile test – fracture surface)

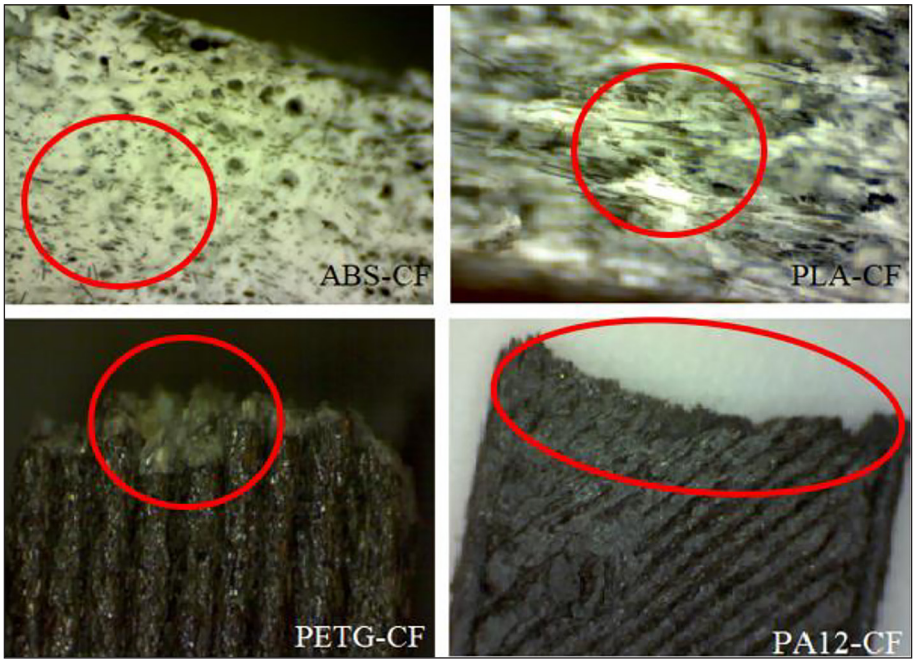

Figure 25. Microscopic imaging of composite polymer samples (after tensile test – fracture surface); black threads of carbon fiber visible

Non-destructive testing results

Microscopic images

The results of microscopic imaging of tensile test specimens are presented in Figures 24 and 25. Samples of all materials are presented. The focus was on fracture areas, so it can be compared how different materials look like after fracture caused by tensile stress. Analyzing the microscopic images of CF-filled material specimen, interesting observations can be made regarding the material color. Originally, all the CF polymers in the experiment were black. In the case of PETG-CF and PA12-CF, this is visible in microscopic imagery. However, in the case of ABS-CF and PLA-CF, the color of polymer is white in microscopic image, with black fibers clearly

distinguishable. This is due to the crazing phenomenon, which occurs mostly in amorphous polymers (ABS and PLA), and not in crystalline polymers (PETG and PA12). This is not visible in pure (non-composite) polymers, mostly because ABS and PLA materials selected for the experiments were of white color. However, this phenomenon is confirmed in available literature [60].

Surface roughness testing results

Results of surface roughness tests (measured before destructive test) for the tensile samples are presented in Table 14 and in diagram in Figure 26. Table 15 and Figure 27 present results for the bending test samples. Figures 28 and 29 present juxtapositions of R_a roughness parameter for pairs of materials, illustrating change in roughness after adding carbon fiber to a polymer material, for two types of samples. Analyzing these results, the following observations can be made:

1. For all the materials except PLA, adding carbon fibers had positive effect on measured roughness, reducing it (surface was smoother). For PLA, no changes were observed in the tensile test samples, while bending test samples had higher roughness when dealing with the CF-filled material.
2. Comparing the materials, it can be observed that pure (no composite) PA12 and PETG

Table 14. Surface roughness tensile testing results (λc = 2.5 mm × 2)

Type	R_a [µm]	R_z [µm]	R_q [µm]
ABS	7.371	38.037	8.682
ABS-CF	4.696	29.167	6.021
PLA	9.296	50.359	11.887
PLA-CF	9.119	55.080	11.240
PA12	15.687	87.567	19.817
PA12-CF	7.563	53.639	10.476
PETG	11.747	48.844	13.273
PETG-CF	3.293	23.602	4.106

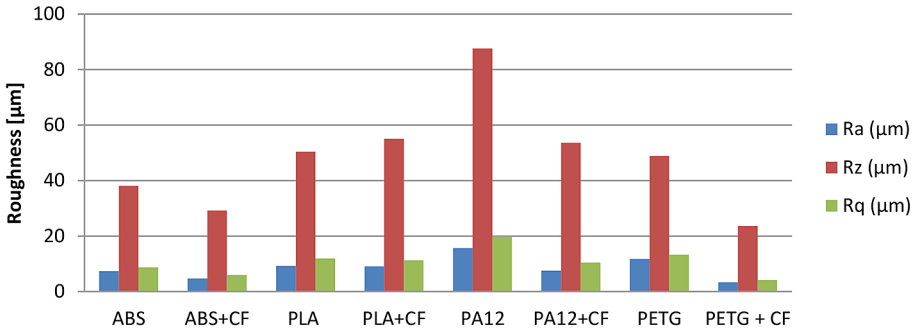

Figure 26. Roughness results of tensile testing

Table 15. Surface roughness bending testing results (λc = 2.5 mm × 2)

Type	R_a [µm]	R_z [µm]	R_q [µm]
ABS	9.198	46.981	10.761
ABS-CF	4.506	27.826	5.469
PLA	8.067	32.521	9.046
PLA-CF	12.218	69.812	15.027
PA12	10.134	47.105	12.138
PA12-CF	5.615	46.757	7.63
PETG	13.615	52.148	15.079
PETG-CF	3.408	21.714	4.226

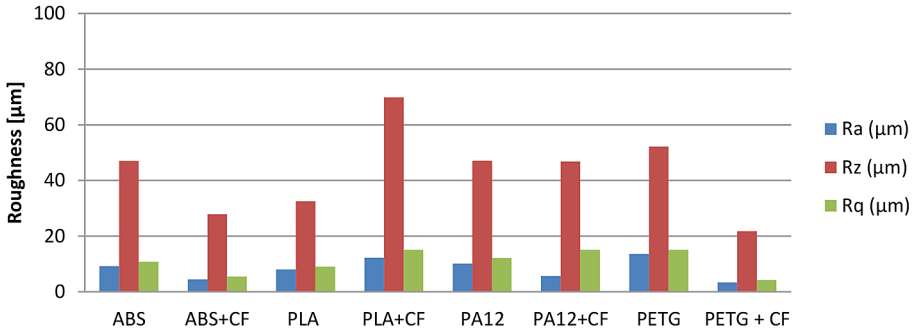

Figure 27. Roughness results of bending testing

have the highest roughness parameters (for both sample types) and they also have the highest roughness reduction after adding carbon fibers to the materials. In direct tactile assessment these two materials were noted as "soft and pleasant" in touch, which is an important observation from the viewpoint of the orthosis 3D printing, as the material will be in skin contact.

3. Comparing the sample types, it can be observed that for the bending test samples, the roughness is generally lower for PA12 and PETG materials. For the ABS and PLA, the roughness of tensile samples is smaller than in the case of bending test samples.

DISCUSSION

It must be emphasized, that in the performed tests, aspect of usability of the material was of highest importance. Less attention was paid to actual phenomena happening in the loaded material, and purely empirical approach was taken, also having in mind application of the tested polymers (production of usable ankle foot orthoses). The discussion towards the obtained and presented results, taking this approach into account, is summarized in the main points, listed below.

1. Of all the tested materials, considering all the recorded material properties, it would be recommended to produce leg orthoses of PA12 and

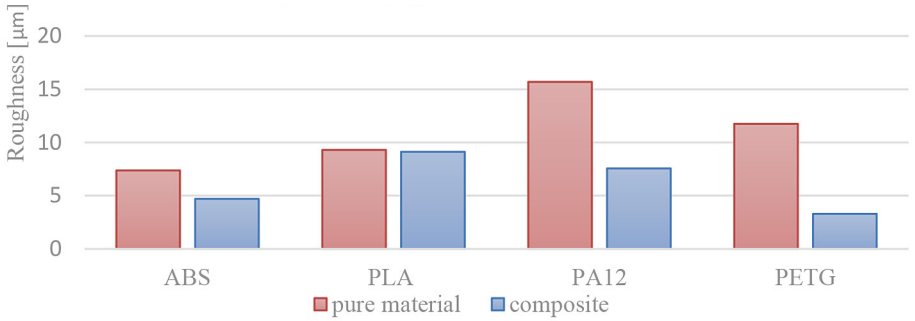

Figure 28. Juxtaposition of Ra roughness parameter (tensile test)

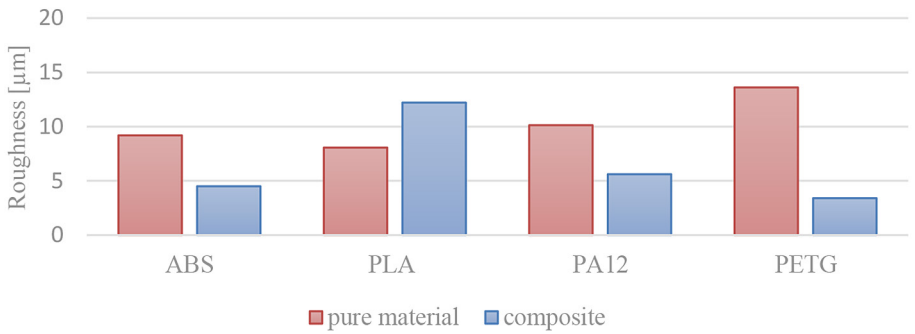

Figure 29. Juxtaposition of Ra roughness parameter (bending test)

PETG carbon fiber composite materials. PETG-CF has the best tensile strength of all materials, best bending strength of all the composite materials and the lowest roughness, meaning less need for polishing before allowing skin contact in use of the orthoses. PA12-CF has also considerably high tensile and bending strengths, highest elongation of all composite materials and a considerably low roughness.

2. Of the pure materials, if no access to composites is possible, PLA is the best choice of material, with high tensile and bending strength and acceptable roughness, with considerably low elongation. However, use of PLA-CF composite is counter effective – obtained properties are worse than in the pure material, while processing is more difficult. This is confirmed by available literature [61].
3. The length of CF fibers depend on the producer, what also affects the strength of the samples. It is also described in the literature [61]. The plasticity of samples with the addition of carbon fibers should decrease slightly, and the strength should increase, but in the case of PLA this has not been confirmed (the second serie also confirmed that the samples have lower strength and higher plasticity), according to the manufacturer, the composite should combine the ease of PLA printing and significantly increased mechanical strength by adding carbon fibers.
4. Considering the processing properties, it would be the most difficult to produce an orthosis using the ABS-CF material. It clogs the nozzles of extruders, disjoints from the machine table during manufacturing and contributes to a very unstable manufacturing process using accessible, low-cost FDM machines (which is the requirement for low-cost and widespread orthosis production, assumed in this paper). Taking into account also the mediocre properties (strength, roughness below of those achieved in the case of PA12 and PETG), it is not recommended to use it in orthosis production via 3D printing.
5. It is worth noting that times of manufacturing are comparable for all the material types, and the simulated times are compatible with real times, at least for the samples of simple geometry. As such, this part of the whole economic factor does not influence the choice of the material. The only difference between pure and CF-filled materials is the price of the material filament itself, as composite filaments are considerably more expensive (almost double the price, considering market availability in mid-2023).
6. The manufacturing of samples with carbon fibers caused clogging of the nozzle. After printing two batches, the nozzle had to be replaced immediately to be able to print samples from subsequent composites. As for pure materials, this problem was not noticed and one nozzle was used to print all ABS, PLA, PETG and PA12 samples.
7. Post-processing is much easier and shorter for carbon-added materials than for pure materials. Raft was removable in a much easier manner, so there was no mechanical damage. However, this is probably caused by weaker adhesion and cohesion in the material in the presence of carbon fibers and it might be a reason behind more difficult manufacturing, with frequent disjoint of the whole printouts from the working table (weaker adhesion of the raft to the table).
8. Samples from PTEG and PA12 with CF were much more pleasant to the touch than out of pure polymer, so it is possible that when making orthoses from these composites, there will be no need to line them with foam, which is a currently accepted and implemented method.

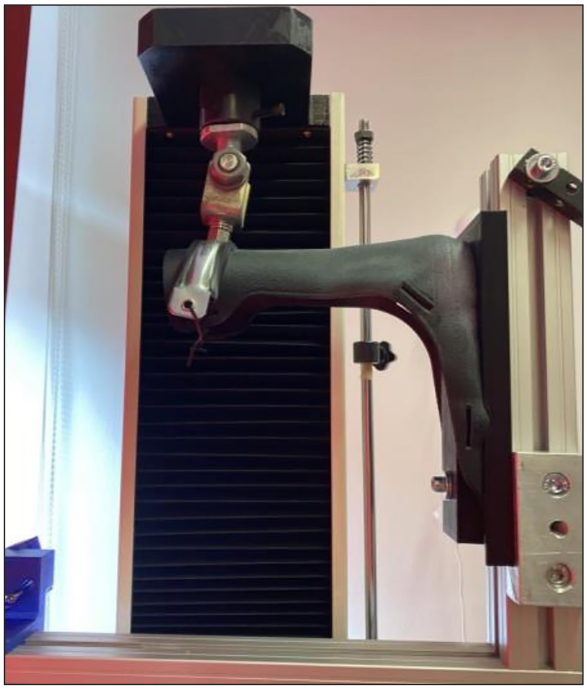

Figure 30. Destructive test of a complete orthosis made of PETG-CF composite filament

CONCLUSIONS

This paper presents results of manufacturing, destructive and non-destructive testing of samples made of pure polymers and the same polymers with added carbon fiber. As such, it was found out how the composite filaments perform in various basic tests as opposed to typical polymer materials used in FDM technology. The results are interesting and sometimes surprising – for typical, popular materials (PLA and ABS) adding carbon fibers can be assessed as counterproductive, basing on the experimental results – the resulting properties are worse or barely comparable, with much higher costs and more troublesome manufacturing. However, for nylon (PA12) and PETG, it was found that adding carbon fibers is a promising direction, as the resulting properties are better.

While evaluating the obtained results, it is also important to consider their weaknesses and limitations. The used filaments were bought commercially – as such, their chemical properties and method of preparation were neither inspected nor controlled. The differences, e.g., in carbon fiber length, or in course of polymerization processes of different suppliers, could influence the visible differences in properties between pure and CF-filled materials. In the future, it would be worth testing composites from other manufacturers and comparing their properties, because they may have longer or shorter fibers, which also affects the strength and plasticity of the samples. It would be also advisable to consider preparing the filaments from the scratch, maintaining full control and similar conditions in the process, to properly and precisely evaluate how adding carbon (and possibly other, like glass) fibers influence the obtained properties. Also, it would be worth testing the materials on various machines. Here only Zortrax 3D printers were used, to maintain similar conditions and parameters – however it would be worth observing how the composite filaments could be processed on various other 3D printers.

The tests were oriented mainly at future production of leg orthoses, as orthoses previously made by the authors of pure polymers were not having sufficient strength properties to sustain prolonged use by teenage or adult patients (they were suitable only for children below age of 13, on average). In the future studies, that have already commenced, instead of samples, whole orthoses will be tested. Partial results of these studies focused on a single material are already described [4]. Tests on full orthoses are presented in Fig. 30. The experiments will be realized in the future as a part of development of the AutoMedPrint system. The search for a proper polymer to endure prolonged use of 3D printed AFO by an adult injured patient will continue, until full functional products will be obtained.

Acknowledgements

The studies were realized with support from the statutory activity financed by the Polish Ministry of Science and Higher Education (0613/SBAD/4771) and Polish National Center for Research and Development in the scope of the "LIDER" program (grant agreement no. LIDER/14/0078/L-8/16/NCBR/2017). The study was conducted in accordance with the Declaration of Helsinki. No human subjects were involved in the experiments.

REFERENCES

1. Górski, F., Kuczko, W., Wichniarek, R., Hamrol, A. Mechanical properties of composite parts manufactured in FDM technology, Rapid Prototyping Journal 2018, 24(8): 1281–1287. https://doi.org/10.1108/RPJ-11-2016-0197
2. Kuczko, W., Hamrol, A., Wichniarek, R., Górski, F., Rogalewicz, M. Mechanical properties and geometric accuracy of angle-shaped parts manufactured using the FFF method, Bulletin of the Polish Academy of Sciences. Technical Sciences 2021, 69(3): e137387. https://doi.org/10.24425/bpasts.2021.137387
3. Lluch-Cerezo, J., Benavente, R., Meseguer, M. D., Gutiérrez, S.C., Study of samples geometry to analyze mechanical properties in Fused Deposition Modeling process (FDM), Procedia Manufacturing 2019, 41: 890–897. https://doi.org/10.1016/j.promfg.2019.10.012
4. Raj, R., Dixit, A.R., Łukaszewski, K., Wichniarek, R., Rybarczyk, J., Kuczko, W., Górski, F. Numerical and Experimental Mechanical Analysis of Additively Manufactured Ankle–Foot Orthoses. Materials 2022, 15: 6130. https://doi.org/10.3390/ma15176130
5. Raj, R., Dixit, A.R. Direct InkWriting of Carbon-Doped Polymeric Composite Ink: A Review on Its Requirements and Applications. 3D Print. Addit. Manufacting 2022. https://doi.org/10.1089/3dp.2021.0209
6. Kurenov, S.N., Ionita, C., Sammons, D., Demmy, T.L.. Three-dimensional printing to facilitate anatomic study, device development, simulation, and

planning in thoracic surgery. Cardiothoracic Surgical Education And Training 2015, 49(4): 973–979. E1

7. Witowski, J.S., Pędziwiatr, M., Major, P., Budzyński, A. Cost-effective, personalized, 3D-printed liver model for preoperative planning before laparoscopic liver hemihepatectomy for colorectal cancer metastases. Int J CARS 2017, 12: 2047–2054.
8. Torres, I.O., De Luccia N. A simulator for training in endovascular aneurysm repair: The use of three dimensional printers. European Journal of Vascular and Endovascular Surgery 2017, 54(2): 247–253.
9. Żukowska, M., Górski, F., Wichniarek, R., Kuczko, W. Methodology of Low Cost Rapid Manufacturing of Anatomical Models with Material Imitation of Soft Tissues. Advances in Science and Technology Research Journal 2019, 13(4): 120–128.
10. Żukowska, M., Górski, F., Bromiński, G. Rapid Manufacturing and Virtual Prototyping of Presurgery Aids. In: Lhotska, L., Sukupova, L., Lacković, I., Ibbott, G. (eds) World Congress on Medical Physics and Biomedical Engineering, IFMBE Proceedings 2018, 68(3). https://www.mdpi.com/2073-4360/14/19/4086
11. Targonska, S., Dobrzanska-Mizera, M., Wukczyk, M., Rewak-Soroczynska, J., Knitter, M., Dopierała, K., Andrzejewski, J., Wilglusz, R.J. New way to obtain the poly (L-lactide-co-D,L-lactide) blend filled with nanohydroxyapatite as biomaterial for 3D-printed bone-reconstruction implants. European Polymer Journal 2022, 165. https://doi.org/10.1016/j.eurpolymj.2022.110997
12. Górski, F., Rybarczyk, J., Zawadzki, P., Kuczko, W., Wierzbicka, N., Żukowska, M., Siwiec, S. Design and additive manufacturing of an individualized specialized leg orthosis MANUFACTURING 2022: Advances in Manufacturing III, 31–44, 10.1007/978-3-030-99769-4_3
13. Górski, F., Wichniarek, R., Kuczko, W., Żukowska, M., Lulkiewicz, M., Zawadzki, P. Experimental Studies on 3D Printing of Automatically Designed Customized Wrist-Hand Orthoses. Materials 2020, 13(18): 4091. https://doi.org/10.3390/ma13184091
14. Górski, F., Zawadzki, P., Wichniarek, R., Kuczko, W., Słupińska, S.., Żukowska, M. Automated Design and Rapid Manufacturing of Low-Cost Customized Upper Limb Protheses, Journal of Physics: Conference Series, 2198, https://doi.org/10.1088/1742-6596/2198/1/012040
15. Dal Maso, A., Cosmi, F. 3D-printed ankle-foot orthosis: a design method, Materials Today: Proceedings 2019, 12: 252–261. https://doi.org/10.1016/j.matpr.2019.03.122
16. Chandra, G., Pandey, A. Biodegradable bone implants in orthopedic applications: a review, Biocybernetics and Biomedical Engineering 2020, 40(2): 596–610.. https://doi.org/10.1016/j.bbe.2020.02.003
17. Chaparro-Rico B.D.M., Martinello K., Fucile, S., Cafolla, D. User-Tailored Orthosis Design for 3D Printing with PLACTIVE: A Quick Methodology, Crystals 2021, 11(5): 561. https://doi.org/10.3390/cryst11050561
18. Fafenrot, S., Grimmelsmann, N., Wortmann, M., Ehrmann, A. Three-dimensional (3D) printing of polymer-metal hybrid materials by fused deposition modeling. Materials 2017, 10: 1199. https://doi.org/10.3390/ma10101199
19. Richter, C., Schmülling, S., Ehrmann, A., Finsterbusch, K. FDM printing of 3D forms with embedded fibrous materials. In Design, Manufacturing and Mechatronics, Proceedings of the 2015 International Conference on Design, Manufacturing and Mechatronics (ICDMM2015), Wuhan, China, 17–18 April 2015, Shahhosseini, A.M., Ed., World Scientific: Singapore 2015, 961–969.
20. Gogolewski, D., Bartkowiak, T., Kozior, T., Zmarzły, P. Multiscale analysis of surface texture quality of models manufactured by laser powder-bed fusion technology and machining from 316L steel. Materials 2021, 14: 2794. https://doi.org/10.3390/ma14112794
21. Bochnia, J., Blasiak, M., Kozior, T.A Comparative Study of the Mechanical Properties of FDM 3D Prints Made of PLA and Carbon Fiber-Reinforced PLA for Thin-Walled Applications, Materials 2021, 14(22): 7062. https://doi.org/10.3390/ma14227062
22. Liu, Z., Wang, Y., Wu, B., Cui, C., Guo, Y., Yan, C.A critical review of fused deposition modeling 3D printing technology in manufacturing polylactic acid parts. Int. J. Adv. Manuf. Technol. 2019, 102: 2877–2889.
23. Chen, Q., Boisse, P., Park, C.H., Saouab, A., Bréard, J. Intra/inter-ply shear behaviors of continuous fiber reinforced thermoplastic composites in thermoforming processes. Compos. Struct. 2011, 93: 1692–1703.
24. Allum, J., Gleadall, A., Silberschmidt, V.V. Fracture of 3D-printed polymers: Crucial role of filament-scale geometric features. Eng. Fract. Mech. 2020, 224: 106818. https://doi.org/10.1016/j.engfracmech.2019.106818
25. Tronvoll, S.A., Vedvik, N.P., Elverum, C.W., Welo, T. A new method for assessing anisotropy in fused deposition modeled parts using computed tomography data. Int. J. Adv. Manuf. Technol. 2019, 105: 47–65. https://doi.org/10.1007/s00170-019-04081-7
26. Kozior, T., Mamun, A., Trabelsi, M., Sabantina, L., Ehrmann, A. Quality of the surface texture and mechanical properties of FDM printed samples after thermal and chemical treatment. Stroj. Vestn. J. Mech. Eng. 2020, 105–113. https://doi.org/10.5545/sv-jme.2019.6322
27. Saad, M.S., Nor, A.M., Baharudin, M.E., Zakaria, M.Z., Aiman, A. Optimization of surface roughness

in FDM 3D printer using response surface methodology, particle swarm optimization, and symbiotic organism search algorithms. Int. J. Adv. Manuf. Technol. 2019, 105: 5121–5137. https://doi.org/10.1007/s00170-019-04568-3

28. Turek, P., Budzik, G., Sęp, J., Oleksy, M., Józwik, J., Przeszłowski, Ł., Paszkiewicz, A., Kochmański, Ł., Żelechowski, D. An analysis of the casting polymer mold wear manufactured using PolyJet method based on the measurement of the surface topography. Polymers 2020, 12: 3029. https://doi.org/10.3390/polym12123029
29. Kousiatza, C., Tzetzis, D., Karalekas, D. In-situ characterization of 3D printed continuous fiber reinforced composites: A methodological study using fiber Bragg grating sensors. Compos. Sci. Technol. 2019, 174: 134–141. https://doi.org/10.1016/j.compscitech.2019.02.008
30. Chaudhry, F.N., Butt, S.I., Mubashar, A., Bin Naveed, A., Imran, S.H., Faping, Z. Effect of carbon fibre on reinforcement of thermoplastics using FDM and RSM. J. Thermoplast. Compos. Mater. 2019, https://doi.org/10.1177/0892705719886891
31. Chabaud, G., Castro, M., Denoual, C., Le Duigou, A. Hygromechanical properties of 3D printed continuous carbon and glass fibre reinforced polyamide composite for outdoor structural applications. Addit. Manuf. 2019, 26: 94–105. https://doi.org/10.1016/j.addma.2019.01.005
32. Bochnia, J., Blasiak, M., Kozior, T. Tensile strength analysis of thin-walled polymer glass fiber reinforced samples manufactured by 3D printing technology. Polymers 2020, 12: 2783. https://doi.org/10.3390/polym12122783
33. Yi, X., Tan, Z.-J., Yu, W.-J., Li, J., Li, B.-J., Huang, B.-Y., Liao, J. Three dimensional printing of carbon/carbon composites by selective laser sintering. Carbon 2016, 96: 603–607, https://doi.org/10.1016/j.carbon.2015.09.110
34. Ahn, B.-H., Moon, G., Sun, W., Akasofu, S.-I., Chen, G.X. and Park, Y.D. Universal time variation of the Dst index and the relationship between the cumulative AL and Dst indices during geomagnetic storms. Journal of Geophysical Research 2002, 107. https://doi.org/10.1029/2002JA009257
35. Ahn S.H., Baek C., Lee S., Ahn I.S. Anisotropic tensile failure model of rapid prototyping parts - fused deposition modeling (FDM), International Journal of Modern Physics B (IJMPB) 2003, 17(8–9).
36. Ahn S.H., Montero M., Odell D., Roundy S., Wright P.K. Material Characterization of Fused Deposition Modeling (FDM) ABS by Designed Experiments, Proceedings of Rapid Prototyping and Manufacturing Conference, SME 2001.
37. Ahn S.H., Montero M., Odell D., Roundy S., Wright P.K. Anisotropic material properties of fused deposition modeling (FDM) ABS, Rapid Prototyping Journal 2002, 8(4).
38. Pająk E., Górski F., Wichniarek R., Dudziak A, Techniki przyrostowe i wirtualna rzeczywistość w procesach przygotowania produkcji, wyd. Promocja 21, Poznań. 2011.
39. Górski F., Wichniarek R., Andrzejewski J. Wpływ orientacji części na wytrzymałość modeli z ABS wytwarzanych techniką modelowania uplastycznionym tworzywem sztucznym, Przetwórstwo Tworzyw 2012.
40. Bellini A., Guceri S. Mechanical characterization of parts fabricated using fused deposition modeling, Rapid Prototyping Journal 2003, 9(4): 252–264.
41. Caminero, M.A., Chacón, J.M., García-Moreno, I., Rodríguez, G.P. Impact damage resistance of 3D printed continuous fibre reinforced thermoplastic composites using fused deposition modelling, Composites Part B 148 2018, 93–103. https://doi.org/10.1016/j.compositesb.2018.04.054
42. Choo, Y.J., Chang, M.C. Commonly used types and recent development of ankle-foot orthosis: a narrative review. Healthcare 2021, 9: 1046. https://doi.org/10.3390/HEALTHCARE9081046
43. Górski F., Wichniarek R., Kuczko W., Żukowska M., Rybarczyk J., Lulkiewicz M. Evaluation of a Prototype System of Automated Design and Rapid Manufacturing of Orthopaedic Supplies, Advances in Manufacturing III, Biomedical Engineering: Research and Technology Innovations, Industry 4.0 2022, 1–15, https://doi.org/10.1007/978-3-030-99769-4_1
44. Górski F., Rybarczyk J., Zawadzki P., Kuczko W., Wierzbicka N., Żukowska M., Siwiec S. Design and Additive Manufacturing of an Individualized Specialized Leg Orthosis, Advances in Manufacturing III, Volume 5 - Biomedical Engineering: Research and Technology Innovations, Industry 4.0 2022, 31–44. https://doi.org/10.1007/978-3-030-99769-4_3
45. Górski F., Osiński F., Żukowska M., Wierzbicka N. Environmental Impact of Additive Manufacturing for Individual Supplies, Advanced Manufacturing Processes II, Springer 2021, 384– 393.
46. Shahar, F.S., Sultan, M.T.H., Shah, A.U.M., Safri, S.N.A., A Comparative Analysis be-tween Conventional Manufacturing and Additive Manufacturing of Ankle-Foot Orthosis | Applied Science and Engineering Progress. Applied Science and Engineering Progress 2020, 13: 96–103. https://doi.org/10.14416/j.asep.2020.03.002
47. Chen R.K., Jin Y., Wensman, J., Shih, A. Additive manufacturing of custom orthoses and prosthese – a review. Additive Manufacturing 2016, https://doi.org/10.1016/J.ADDMA.2016.04.002
48. Fox, J.R., Lovegreen W. Lower limb orthoses. Atlas of Orthoses and Assistive

Devices 2019, 239–246. https://doi.org/10.1016/B978-0-323-48323-0.00022-6

49. Kabir, R., Sunny, Md., Ahmed, H., Rahman, M. Hand rehabilitation devices: a comprehensive systematic review, Micromachines 2022, 13(7): 1033. https://doi.org/10.3390/mi13071033
50. Tagliaferri, V., Trovalusci, F., Guarino, S., Venettacci, S. Environmental and economic analysis of FDM, SLS and MJF additive manufacturing technologies, Materials 2019, 12: 4161. https://doi.org/10.3390/ma12244161
51. Love, L.J., Kunc, V., Rios, O., Duty, C.E., Elliott, A.M., Post, B.K., Smith, R.J., Blue, C.A. The importance of carbon fiber to polymer additive manufacturing. J. Mater. Res. 2014, 29: 1893.
52. Rijckaert, S., Daelemans, L., Cardon, L., Boone, M., Paepegem, W.V., De Clerck, K. Continuous fiber-reinforced aramid/PETG 3D-printed composites with high fiber loading through fused filament fabrication, Polymers 2022, 14(2): 298. https://doi.org/10.3390/polym14020298
53. Tambrallimath, V., Keshavamurthy, R., Bavan, S.D., Patil, A.Y., Yunus Khan, T.M., Badruddin, I.A., Kamangar, S. Mechanical Properties of PC-ABS-Based Graphene-Reinforced Polymer Nanocomposites Fabricated by FDM Process, Polymers 2021, 13(17): 2951. https://doi.org/10.3390/polym13172951
54. Tobalina-Baldeon, D., Sanz- Adán, F., Martinez-Calvo, M., Gomez, C., Sanz-Pena, I., Cavasa, F. Feasibility Analysis of Bolted Joints with Composite Fibre-Reinforced Thermoplastics, Polymers 2021, 13(12): 1904. https://doi.org/10.3390/polym13121904
55. Musioł, M., Rydz, J., Janeczek, H., Kordyka, A., Andrzejewski, J., Sterzyński, T., Jurczyk, S., Cristea, M., Musiol, K., Kampik, M., Kowalczuk, M. (Bio)degradable biochar composites -Studies on degradation and electrostatic properties, Materials science and engineering: B 2022, 275: 115515,. https://doi.org/10.1016/j.mseb.2021.115515
56. Wei, S., Ma, J-X., Xu, L., Gu, X-S., Ma, X-L. Biodegradable materials for bone defect repair, Military Medical Research 2020, 7(54).
57. Farah, S., Anderson, D. G., Langer, R. Physical and mechanical properties of PLA, and their functions in widespread applications — A comprehensive review, ADR-13025; 26, https://doi.org/10.1016/j.addr.2016.06.012
58. Kumar, V., Ahuja, I.S., Singh, R. Multi-Factor Optimization for Preparation of mechanical blended and chemical assisted mechanical blended ABS-graphene composite for 3D printing, Encyclopedia of Materials: Plastics and Polymers 2022, 1: 281–287. https://doi.org/10.1016/B978-0-12-820352-1.00216-9
59. Touris, A., Turcios, A., Mintz, E., Pulugurtha, S.R., Thor, P., Jolly, M., Jalgaonkar, U. Effect of molecular weight and hydration on the tensile properties of polyamide 12. Results Mater. 2020, 8: 100149. https://doi.org/10.1016/j.rinma.2020.100149
60. Conway, K.M., Pataky, G.J. Crazing in additively manufactured acrylonitrile butadiene styrene. Engineering Fracture Mechanics 2019, 211: 114–124.
61. Maqsood, N., Rimašauskas, M. Characterization of carbon fiber reinforced PLA composites manufactured by fused deposition modeling. Composites Part C: Open Access 2021, 4: 100112.
62. Istrate, B., Munteanu, C., Antoniac, I., Lupescu, S. Current research studies of Mg–Ca–Zn biodegradable alloys used as orthopedic implants—review, Crystals 2022, 12(10): 1468. https://doi.org/10.3390/cryst12101468
63. Standard Terminology for Additive Manufacturing Technologies. ASTM International; West Conshohocken, PA, USA: 2012. [Google Scholar]
64. Kłonica, M., Analysis of the effect of selected factors on the strength of adhesive joints, 2018 IOP Conf. Ser.: Mater. Sci. Eng. 393 012041, https://doi.org/10.1088/1757-899X/393/1/012041
65. Skoczylas, J., Kłonica, M., Samborski, S. A study on the FRP composite's matrix damage resistance by means of elastic wave propagation analysis, Composite Structures 2022, 297: 115935. https://doi.org/10.1016/j.compstruct.2022.115935